XXIII IMEKO World Congress "Measurement: sparking tomorrow's smart revolution"
August 30 – September 3, 2021, Yokohama, Japan

PROGRESS TOWARDS COMPARISON OF QUANTUM AND CLASSICAL VACUUM STANDARDS

D. S. Barker [a, *], *N. N. Klimov* [a], *E. Tiesinga* [b], *J. A. Fedchak* [a], *J. Scherschligt* [a], *S. Eckel* [a]

[a] Sensor Science Division, National Institute of Standards and Technology, Gaithersburg, MD, USA
[b] Quantum Measurement Division, National Institute of Standards and Technology, Gaithersburg, MD, USA
* Corresponding author. E-mail address: daniel.barker@nist.gov

Abstract – We present our progress towards a comparison of NIST's cold atom primary vacuum standard and a dynamic expansion vacuum standard. The cold atom vacuum standard (CAVS) converts the loss rate of atoms from a magnetic trap to a vacuum pressure using *ab initio* calculations of the quantum atom-molecule collision cross-section. To validate the CAVS, we have constructed a new flowmeter and dynamic expansion system that can produce low-uncertainty pressures in the ultra-high-vacuum range that is required for atom trapping. We discuss the operation and systematics of both the CAVS and flowmeter.

Keywords: vacuum metrology, laser cooling, atom-molecule scattering

1. INTRODUCTION

Many scientific fields and industrial applications require vacuums in the UHV (10^{-7} Pa to 10^{-10} Pa) or XHV (less than 10^{-10} Pa) regime. For example, collisions with background gas molecules limit the number of qubits in some quantum computer architectures [1] and are a source of systematic uncertainty in optical clocks [2]. Residual gas in electron accelerators causes back-bombardment of the electron-beam generating photocathodes, leading to significant maintenance downtime [3]. Molecular-beam epitaxy requires a pristine vacuum environment to prevent unacceptable impurity levels in the resulting crystal [4].

The preparation and measurement of XHV and UHV environments has been complicated by the lack of primary standards for these pressure ranges [5]. Recently, laser-cooled atomic gases have been proposed as primary sensors of vacuum pressure and initial tests of these new sensors have been promising [5-8]. However, high-precision comparisons of cold-atom vacuum sensors to dynamic expansion standards are needed.

2. OPERATION OF THE CAVS

The background gas induced loss rate Γ of sensor atoms from a trap is given by

$$\Gamma = P\langle v\sigma\rangle/k_B T, \qquad (1)$$

for a background gas with pressure P, temperature T, relative velocity v, and collision cross section σ (the brackets denote a thermal average and k_B is Boltzmann's constant). We measure Γ by monitoring the exponential decay of the sensor atom population within the trap. We then invert Eq. (1) to extract the background gas pressure. The thermally averaged loss rate coefficient $\langle v\sigma\rangle$ has been calculated using first principles quantum scattering theory for Li-H_2 and Li-He collisions [9, 10], motivating us to choose lithium as our primary sensor atom. We will extend to other background gasses and other possible sensor atoms, like rubidium, by measuring relative sensitivity coefficients in a combined CAVS and dynamic expansion system [5].

To determine the range of operation of the CAVS, we need to characterize additional loss processes present in the magnetic trap. The density of sensor atoms n_s in the trap decays as

$$\dot{n}_s = -\Gamma n_s - \Gamma_m n_s - K_{ev} n_s^2 - K_2 n_s^2 - K_3 n_s^3, \qquad (2)$$

where the coefficients Γ_m, K_{ev}, K_2, and K_3 characterize spin-flip loss, evaporation, dipolar relaxation, and 3-body recombination, respectively. Evaporative, dipolar, and 3-body losses depend nonlinearly on the density of sensor atoms and can be eliminated by using a low-density sensor ensemble. Spin-flip losses depend on the details of the magnetic trap and can be suppressed by using a trap design that has a nonzero bias magnetic field at its center [11, 12].

One trap design provides a nonzero magnetic bias field is Ioffe-Pritchard trap. We choose a Ioffe-Pritchard trap for the CAVS because it is both easily tunable and uses only static magnetic fields. Our Ioffe-Pritchard trap has a cloverleaf winding pattern and consists of three independent electromagnets: the curvature coil, the antibias coil, and the cloverleaf coil [12]. The curvature coil provides axial confinement and supplies most of the bias field. The antibias coil is a Helmholtz coil that partially nulls the bias field from the curvature coil. Together, these coils allow independent control of the axial confinement and bias field. The cloverleaf coil traps the sensor atoms radially and, due to a quirk of our coil winding pattern, also produces a small contribution to the bias field.

Fig. 1 shows the decay of rubidium atoms confined in the CAVS using either a Ioffe-Pritchard trap (blue circles) or a quadrupole trap (red circles), which has a magnetic field zero at its center. Both decay curves are well-described by an exponential fit (gray lines in Fig. 1). The quality of the fits indicates that we have prepared a low-density sample of

sensor atoms, suppressing evaporation, dipolar relaxation, and 3-body recombination. Because the vacuum conditions were the same for both decay curves in Fig. 1, we attribute faster loss of atoms from the quadrupole trap to non-adiabatic spin-flips near the magnetic field zero. The measured loss rate from the Ioffe-Pritchard trap is $\Gamma = 4.3(2) \times 10^{-3}$ s^{-1} at a bias field of approximately 200 μT. (Here, and throughout the paper, parenthetical quantities represent the standard error). Applying the calibration coefficient of Ref. [7] to Γ yields a vacuum pressure on the order of 10^{-9} Pa.

Glancing (or quantum diffractive) collisions are another important correction to operation of the CAVS [6, 11]. Eq. (1) assumes that every collision between a background gas molecule and a sensor atom ejects that atom from the trap. However, the assumption that each collision ejects an atom is violated when the background gas molecule does not transfer kinetic energy exceeding the energy needed to the escape the trap (the trap depth) to the sensor atom. The effect of glancing collisions can be captured by replacing $\langle v\sigma \rangle$ in Eq. (1) with an effective loss rate coefficient $\langle K_{CAVS} \rangle = \langle v\sigma \rangle - \langle K_{gl} \rangle$, where $\langle K_{gl} \rangle$ is the thermally averaged glancing collision rate coefficient. To accurately compare the CAVS to a dynamic expansion flow standard, we must know the depth of the magnetic trap, so that we can calculate the correction $\langle K_{gl} \rangle$ (or ensure that it is negligible compared to other sources of uncertainty).

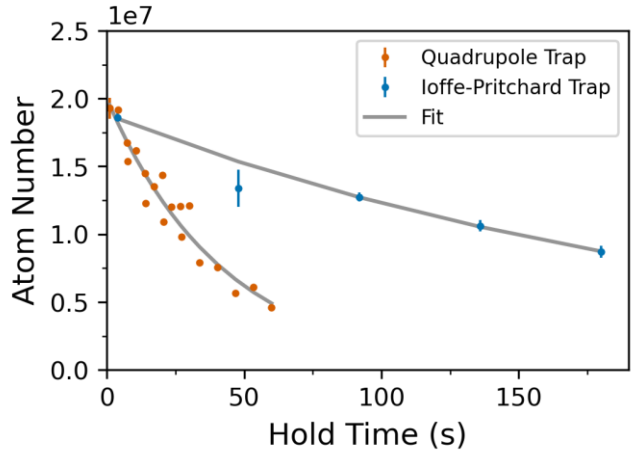

Fig. 1. Loss of rubidium atoms from a quadrupole trap (red circles) and Ioffe-Pritchard trap (blue circles) as a function of time. Gray lines show exponential fits to the data. Errorbars on the Ioffe-Pritchard trap data, and first data point for the quadrupole trap, represent the standard error and are often smaller than the data points.

The depth of a Ioffe-Pritchard trap is set by two parameters: the bias field at the trap center and the frequency of an applied radiofrequency (RF) magnetic field. The bias field sets the magnetic potential energy $\mu_B B/2$ of a stationary sensor atom at the center of the trap, where μ_B is the Bohr magneton and B is the magnetic field. When an atom moves away from the center of the trap, its magnetic potential energy increases and it comes into resonance with the RF magnetic field. The RF magnetic flips the spin of the sensor atom, ejecting it from the trap. The difference between the resonant potential energy of the RF field and potential energy of the bias field is the Ioffe-Pritchard trap depth.

The uncertainty in the CAVS magnetic trap depth is dominated by uncertainty in the Ioffe-Pritchard trap bias field. To measure the bias field, we sweep the frequency of the RF magnetic field while monitoring number of trapped sensor atoms and the shape of the trapped atom cloud. By sweeping the RF field from low frequency to high frequency, we trigger atom loss when RF comes into resonance with sensor atoms at the trap center, where their magnetic potential energy is given by the bias field. Fig. 2 shows the RF resonance frequency at the trap center as function of current applied to each of the antibias coil (top), cloverleaf coil (middle), and curvature coil (bottom). The typical standard error of the resonance frequency measurements is 30 kHz, which corresponds to a bias field uncertainty of approximately 4 μT. The achieved bias field uncertainty is sufficient for our comparison of the CAVS to a dynamic expansion flow standard.

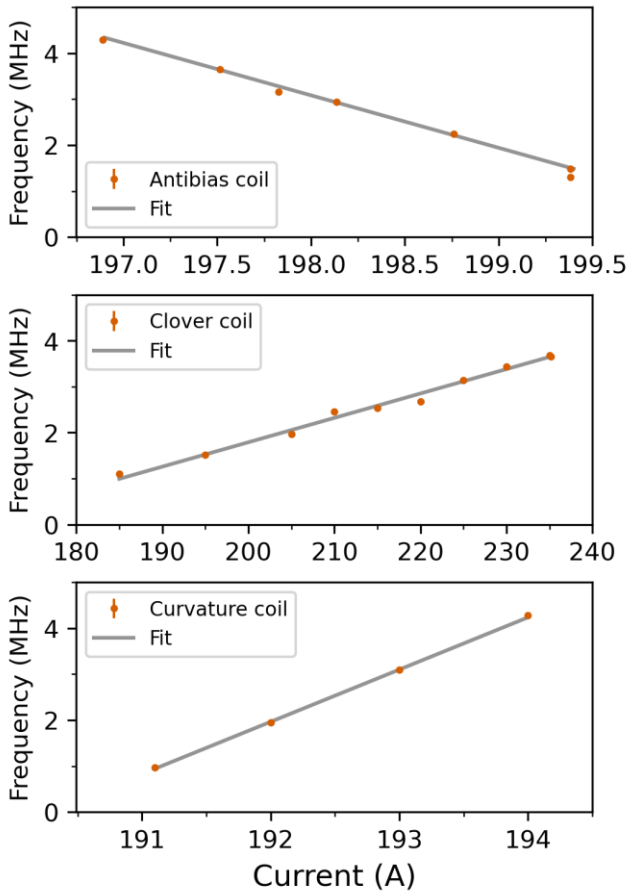

Fig. 2. Ioffe-Pritchard trap bias field characterization. We show the RF field resonance frequency at the trap center (red circles) as function of current applied to the antibias coil (top), cloverleaf coil (middle), and curvature coil (bottom). Gray lines are linear fits to the data. Errorbars indicate the standard error and are usually smaller than the data points.

We further characterize our Ioffe-Pritchard trap by performing linear fits on the data in Fig. 2. The slope of the fit allows us to extract the bias magnetic field produced per ampere of current in each coil. The results for the curvature coil, antibias coil, and cloverleaf coil are 162(3) μT/A, -163(5) μT/A, 7.6(2) μT/A, respectively. Our present measurements of the applied bias field per ampere are larger

than prior offline measurements using a Hall probe [12]. Agreement with the Hall probe measurements occurs at the 2σ, 1σ, and 3σ level for the curvature coil, antibias coil, and cloverleaf coil, respectively. The level of agreement between our present and prior measurements suggests that dimensional relaxation may be occurring in our Ioffe-Pritchard electromagnets. However, we made the Hall probe measurements in 2018 and the data in Fig. 2 was collected in 2021. The dimensional drift of the Ioffe-Pritchard trap is therefore negligible on the anticipated several month duration of the comparison between the CAVS and the dynamic expansion flow standard.

3. COMPARISON TO CLASSICAL STANDARD

The CAVS is paired with a new dynamic expansion flow standard both for metrological testing and measuring relative sensitivity coefficients. Our dynamic expansion system contains a precision 22 mm orifice, yielding approximately 40 L/s conductance for N_2. The associated XHV flowmeter can produce flows as low as 10^{-13} mol/s for N_2, producing partial pressures of the order of 10^{-8} Pa, compatible with atom trapping, in the dynamic expansion chamber. We have demonstrated the flowmeter's performance via helium flow comparison with NIST's existing low-range standard flowmeter [13]. The details of the comparison of the XHV flowmeter to NIST's low-range standard will be the subject of a future publication.

We have begun initial testing of the combined CAVS and dynamic expansion flow standard. During the initial tests, we use rubidium atoms in the CAVS because they are easier to prepare in the Ioffe-Pritchard trap than lithium atoms. Fig. 3 shows the decay of rubidium atoms from the Ioffe-Pritchard trap for several He gas flows on a semilog scale. The Ioffe-Pritchard trap bias field for the data in Fig. 3 is approximately 100 μT and RF field frequency is fixed at 40 MHz, so the trap depth corresponds to a temperature of approximately 2 mK. Because the bias field is lower than in Fig. 1, spin-flip losses are not negligible and background loss rate from the trap (blue circles in Fig. 3) is $\Gamma = 7.7(6) \times 10^{-3}$ s^{-1}. When the XHV flowmeter supplies helium to the dynamic expansion chamber that is connected to the CAVS, the loss rate from the trap increases dramatically. For He flows of 3×10^{-12} mol/s and 6×10^{-12} mol/s, the loss rates are $\Gamma = 4.60(2) \times 10^{-2}$ s^{-1} and $\Gamma = 8.7(2) \times 10^{-2}$ s^{-1}, respectively. Losses due to Rb-He collisions dominate background losses despite the relatively modest He partial pressure, which is on the order of 10^{-8} Pa.

We were not monitoring the temperature of the CAVS vacuum chamber while collecting the data in Fig. 3. We will need accurate measurements of the helium gas temperature in the CAVS chamber to apply Eq. (1) to the loss rate measurements and extract a value for the Rb-He loss rate coefficient $\langle v\sigma \rangle$. A suite of platinum resistance thermometers (PRT) is currently being installed on both the CAVS vacuum chamber and the dynamic expansion system. Once the PRT installation is complete, we will know both the temperature and partial pressure of the helium gas at the Ioffe-Pritchard trap. We can then use Eq. (1) to compare our classical dynamic expansion flow standard to the CAVS using Rb-He loss rate coefficient measurement of Ref. [6].

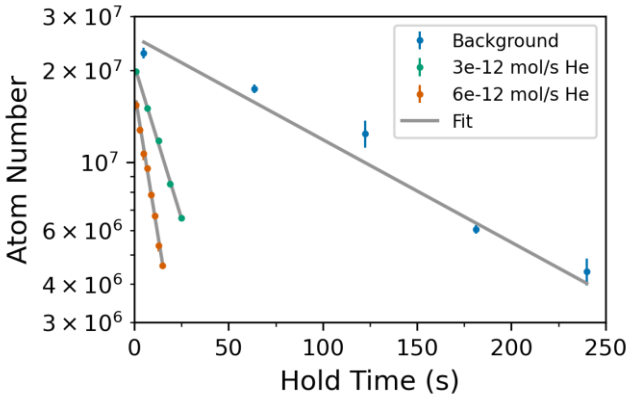

Fig. 3. Loss of rudidium atoms trapped in the CAVS as a function of time for several helium gas flows. Blue circles show the background gas induced decay. Green and red circles show the decay with He flows of 3×10^{-12} mol/s and 6×10^{-12} mol/s, respectively. Gray lines are exponential fits to each decay curve. Errorbars represent the standard error and are usually smaller than the data points.

3. CONCLUSIONS

We have presented our progress towards high precision comparisons of quantum and legacy pressure standards. Diagnostics of our Ioffe-Pritchard magnetic trap show that we can suppress or control measurement systematics related to the dynamics of the sensor atoms within the trap. We anticipate that precision of the standards comparison will be limited by dynamic expansion flow standard and not the CAVS. Initial measurements of helium-induced loss rates demonstrate that the XHV flowmeter and dynamic expansion system can produce stable pressures that are compatible with CAVS. After PRTs are installed on the CAVS and dynamic expansion system, full validation of the standards comparison apparatus will commence.

Thus far, first principles quantum scattering calculations of $\langle v\sigma \rangle$ are only available for Li-H_2 and Li-He collisions [9, 10]. Because the first principles calculations establish the CAVS as a quantum pressure standard, measurements of H_2-induced and He-induced loss of lithium atoms from the CAVS magnetic trap must be made for a full comparison of the CAVS and dynamic expansion system. The CAVS can load either lithium or rubidium into its Ioffe-Pritchard trap. Once we have certified the performance of the standards comparison apparatus using rubidium sensor atoms, we will begin comparisons of the CAVS and dynamic expansion flow standard with lithium sensor atoms. Such comparisons are necessary to validate the performance of quantum standards and realize their full metrological potential.

ACKNOWLEDGMENTS

This research was funded by the National Institute of Standards and Technology.

REFERENCES

[1] G. Pagano et al, *Cryogenic trapped-ion system for large scale quantum simulation*, Quantum Science and Technology 4, 014004, 2019.

[2] A.M. Hankin et al, *Systematic uncertainty due to background-gas collisions in trapped-ion optical clocks*, Physical Review A 100, 033419, 2019.
[3] M.L. Stutzman, P. Adderley, J. Grames, M. Poelker, K. Surles-Law, *DC photogun vacuum characterization through photocathode lifetime studies*, Journal of Physics: Conference Series 100, 092016, 2008.
[4] G. Biasiol, L. Sorba, in *Crystal growth of materials for energy production and energy-saving applications*, edited by R. Fornari and L. Sorba (Edizioni ETS, Pisa, 2001) pp. 66-83.
[5] J. Scherschligt et al, *Development of a new UHV/XHV pressure standard (cold atom vacuum standard)*, Metrologia 54, S125, 2017.
[6] P. Shen, K.W. Madison, J.L. Booth, *Realization of a universal quantum pressure standard*, Metrologia 57, 025015, 2020.
[7] T. Arpornthip, C.A. Sackett, K.J. Hughes, *Vacuum-pressure measurement using a magneto-optical trap*, Physical Review A 85, 033420, 2012.
[8] V.B. Makhalov, K.A. Martiyanov, A.V. Turlapov, *Primary vacuometer based on an ultracold gas in a shallow optical dipole trap*, Metrologia 53, 1287, 2016.
[9] C. Makrides et al, *Elastic rate coefficient in $Li+H_2$ collisions in the calibration of a cold-atom vacuum standard*, Physical Review A 99, 042704, 2019.
[10] C. Makrides et al, *Collisions of room-temperature helium with ultracold lithium and the van der Waals bound state of HeLi*, Physical Review A 101, 012702, 2020.
[11] D.E. Fagnan et al, *Observation of quantum diffractive collisions using shallow atomic traps*, Physical Review A 80, 022712, 2009.
[12] J.L. Siegel, D.S. Barker, J.A. Fedchak, J. Scherschligt and S. Eckel, "A Bitter-type electromagnet for complex atomic trapping and manipulation" *Review of Scientific Instruments* **92**, 033201 (2021).
[13] K.E. McCulloh, C.R. Tilford, C.D. Ehrlich, and F.G. Long, "Low-range flowmeters for use with vacuum and leak standards" *Journal of Vacuum Science & Technology A: Vacuum, Surfaces, and Films* **5**, 376 (1987).